

## Detection and Parameter Estimation of LFM Signal Based on Stochastic Resonance

Xiaomin Wang<sup>1</sup> and Chuan Wen<sup>2</sup>

Key Lab of Traffic Information Engineering and Control, Southwest Jiaotong University, Chengdu, China

<sup>1</sup>xmwang@home.swjtu.edu.cn, <sup>2</sup>wenchuan351@126.com

**Abstract**—This paper presents a novel approach for the detection and parameter estimation of weak linear frequency modulated (LFM) signal based on Stochastic Resonance (SR). By correlating the segmented equal-length LFM signals, the aperiodic LFM signal is transformed into periodic signal which is then input into SR system to estimate the chirp rate of LFM signal. The initial frequency, based on the reconstruction of LFM signal with estimated chirp rate, is further estimated by spectrum averaging technique. The detection probability and parameter estimation accuracy with respect to signal-to-noise ratio (SNR) are evaluated. Simulation experiments show that the proposed method can effectively detect LFM signal in very low SNR environment.

**Keywords**-Linear frequency modulated signal (LFM); Stochastic Resonance (RS); Weak signal detection; Parameter estimation

### 1. Introduction

Linear frequency modulated (LFM) signal, also known as chirp signal, is a kind of classic non-stationary signal widely used in wireless communication, radar, sonar and ultrasound systems [1]. Detection and estimation chirp rate and initial frequency of LFM signals in a noisy environment is of great importance, and it has been the research hotspot in the last two decades.

Utilizing the clustering characteristics of LFM signals in time-frequency plane, a class of parameter estimation methods based on time-frequency analysis (TFA) were proposed, such as Radon-Ambiguity transform[1], Wigner-Hough transform (WHT)[2], Hough transform with short-time Fourier analysis[3], fractional Fourier transform (FRFT)[4], and Hilbert-Huang Hough Transform[5], etc. Recently, G. Bi et al.[6] presented a method to detect LFM signals by jointly using local polynomial periodogram and Hough transform (LPP-HT). The algorithm achieves significant improvement on detecting the LFM signals in low signal-to-noise ratio (SNR) environments. X. Lv et al.[7] studied the LFM signals detection using keystone transformation of Wigner-Ville distribution. The processing eliminates the effects of linear frequency migration to all signal components whereas the computational complexity is up to  $O(4N^2 \log_2^N)$ . Most of these methods can be ascribed to multivariable optimization algorithm whose accuracy is closely related to the grid solution of the search procedure. Heavy computational complexity is generally needed for high estimation accuracy. Moreover, these algorithms are usually invalid at the case of very low SNR.

Recently, Stochastic Resonance (SR) phenomenon has been extensively paid attention to weak periodic signal and mechanical fault detections [8-11]. The detection principle is that SR possesses excellent noise suppression property through the way of transferring noise energy to signal energy and thus enhances the SNR of system output. Based on such principle of SR, this paper proposes a novel approach to detection aperiodic LFM signals at very low SNR condition. In the proposed algorithm, the noise corrupted LFM signal is first segmented into multi-section signals with equal length, which are processed by correlating, phase compensating and smooth filtering sequentially to obtain periodic signal. Then the periodic signal is input into

SR system for chirp rate estimation and the initial frequency is further estimated by spectrum averaging technique. The detection probability and parameter estimation accuracy are evaluated. Moreover, the detection performance with respect to segmentation number of smooth filtering is tested. Simulation results show that the proposed algorithm can detect and estimate LFM signal relatively accuracy even at the case of SNR=-20dB, which outperforms the time-frequency based algorithms.

The rest of this paper is organized as follows. Section II describes the basic principle of SR. Section III presents the detection and parameter estimation algorithm of LFM signal. Section IV gives the numerical simulations. Section V comes to the conclusion.

## 2. The SR of Simple Bistable System

SR phenomenon was first introduced by Benzi et al.[8] and has been experimentally observed in various bistable systems. The simple bistable system extensively exploited in the study of SR is Langevin equation as:

$$dx / dt = ax - bx^3 + A\cos(2\pi ft) + n(t) \quad (1)$$

where  $a>0$ ,  $b>0$  are system parameters,  $A$  is the periodic signal amplitude with frequency  $f$ .  $n(t)$  is zero-mean white gaussian noise (WGN), with an autocorrelation function given by  $E[n(t)n(t+\tau)] = 2D\delta(t-\tau)$  where  $D$  is noise intensity.

Let  $V(x)$  denote the potential function of Eq.(1), we have

$$V(x) = -\frac{1}{2}ax^2 + \frac{1}{4}bx^4 - x(A\cos(2\pi ft) + n(t)) \quad (2)$$

when  $A=D=0$ , Eq.(2) has two stable states  $x_m = \pm(a/b)^{1/2}$  and one unstable state  $x=0$ . The barrier height of the potential is  $\Delta U = a^2 / 4b$ . The potential minimums are located at  $x_m = \pm(a/b)^{1/2}$ . Now the system state is restricted in the one of these two potential minimums, and decided by the initial conditions. When  $A < A_c = (4a^3/27b)^{1/2}$ , two potential minimums take transformation of opposites, and the potential energy deflect according to the frequency of the signal. When  $D \neq 0$  and it reaches a certain value, with the synergistic effect of the signal and noise, the particle turns between two points ( $\pm x_m$ ) with frequency  $f$ . Because the voltage difference between two points ( $\pm x_m$ ) is much larger than the amplitude of the input, the output signal is amplified. This phenomenon is referred to stochastic resonance.

On the other hand, when  $t_0 \rightarrow \infty$  asymptotically, the memory of the initial conditions gets lost and mean value of  $x(t)$  becomes a periodic function of time as follows:

$$E\{x(t)\} = X \sin(2\pi ft - \varphi) \quad (3)$$

where

$$X = \frac{AE\{x^2\}}{D} \frac{r_k}{\sqrt{r_k^2 + (\pi f)^2}} \quad (4)$$

$$\varphi = \arctan\left(\frac{\pi f}{r_k}\right) \quad (5)$$

$$r_k = \frac{1}{\sqrt{2\pi}} \exp\left(-\frac{\nabla U}{D}\right) \quad (6)$$

Here  $r_k$  is Kramers rate,  $E\{x^2\} = x_m^2$  in the case of two states. From Eq.(4) the amplitude  $X$  first increases to a maximum with respect to noise level, and then decreases again. Figure 1 depicts the celebrated SR effect.

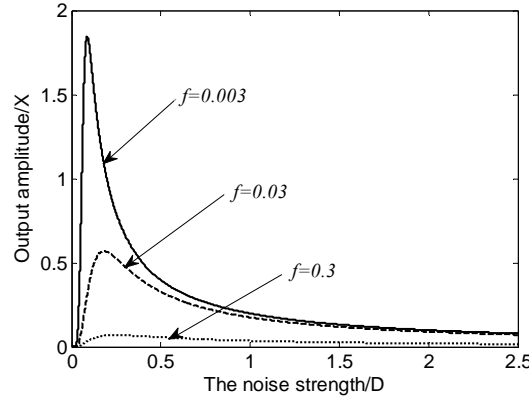


Figure 1. The periodic response amplitude  $X$  vs. the noise strength  $D$  for different frequency  $f$  when  $A=0.2$ ,  $a=1$ ,  $b=1$  in Eq.(4).

### 3. The Detection of Lfm Signal Based on Sr

Consider a noise corrupted LFM signal as

$$z(t) = s(t) + n(t) = A \exp(j2\pi(f_0 t + \frac{k}{2} t^2)) + n(t), \quad (7)$$

where  $A$  is amplitude of LFM signal,  $k$  the chirp rate,  $f_0$  the initial frequency, and  $n(t)$  the zero-mean white Gaussian complex noise.

To estimate  $k$  and  $f_0$  in Eq.(7) in the case of low SNR, we utilize the segmented correlation smoothing method on LFM to obtain the segmented periodic signals for chirp rate estimation based on SR, and then the frequency spectrum averaging is employed to get the initial frequency estimation. The detailed algorithm is described as follows.

**Step 1.** Divide  $z(t)$  into  $M$  segments and the length of every segment is  $T$ . The conjugated product of the  $m$ th segment and the  $(m+1)$ th segment is defined as

$$\begin{aligned} c_m(t) &= z(t - mT) \times z^*(t - (m+1)T) \\ &= A^2 \exp(j2\pi(f_0 T - \frac{2m+1}{2} kT^2 + kTt)) + p_m(t), \end{aligned} \quad (8)$$

$$m = 0, 1, 2, \dots, M-2$$

where  $p_m(t)$  can be regarded equivalently as noise.

**Step 2.** Forward  $c_m(t)$  with  $mT$  units to compensate its phase, and denote the phase-compensated signal as  $c'_m(t)$ . It is not surprise that all the  $c'_m(t)$  s have the same initial phase ( $f_0 T - \frac{1}{2} kT^2$ ), irrelevant with  $m$ .

$$\begin{aligned} c'_m(t) &= c_m(t + mT) \\ &= A^2 \exp(j2\pi(kTt + kmT^2 + f_0 T - \frac{2m+1}{2} kT^2)) + p_m(t + mT) \\ &= A^2 \exp(j2\pi(kTt + f_0 T - \frac{1}{2} kT^2)) + p_m(t + mT) \end{aligned} \quad (10)$$

**Step 3.** Smooth signal  $c'_m(t)$  for  $m = 0, 1, \dots, M-2$  and get their real parts. By this way, the SNR is effectively improved, and the smoothed signal denoted as  $s_1(t)$  is a standard periodic signal with frequency  $kT$ , noised by  $P_m(t + mT)$ .

$$\begin{aligned} s_1(t) &= \frac{1}{M} \sum_{m=0}^{M-1} \text{Re}(c'_m(t)) \\ &= A^2 \cos(2\pi kTt + f_0 T - \frac{1}{2} kT^2) \\ &\quad + \frac{1}{M} \sum_{m=0}^{M-1} \text{Re}(P_m(t + mT)), \end{aligned} \quad (11)$$

where  $\text{Re}(x)$  denotes taking the real part of  $x$ .

**Step 4.** Input  $s_1(t)$  into Eq.(1), then the frequency  $kT$  of  $s_1(t)$  can be estimated by the spectrum peak of SR. For the purpose of improving the estimation accuracy, spectrum averaging technique can be further utilized. Assume  $\hat{f}$  represent the estimated frequency from SR, it is straightforward that the estimated chirp rate is  $\hat{k} = \hat{f} / T$ .

**Step 5.** Use  $\hat{k}$  to construct a new sequence

$$z_1(t) = \exp(-j\pi\hat{k}t^2) \quad (12)$$

and take the real part of the product of  $z(t)$  and  $z_1(t)$  as

$$\begin{aligned} g(t) &= \text{Re}(z(t) \times z_1(t)) \\ &= A \cos\left(2\pi\left(f_0t + \frac{k - \hat{k}}{2}t^2\right)\right) + \text{Re}\left(\exp(-j\pi\hat{k}t^2)n(t)\right) \\ &\approx A \cos(2\pi f_0t) + \text{Re}\left(\exp(-j\pi\hat{k}t^2)n(t)\right) \end{aligned} \quad (13)$$

Eq.(13) shows that  $g(t)$  is a periodic signal with frequency  $f_0$ , the initial frequency of LFM signal, and the last item in Eq.(13) can be regarded as additive noise upon to  $g(t)$ . Since the SNR of  $g(t)$  is higher than that of  $s_1(t)$ , the estimation of initial frequency  $\hat{f}_0$  can be obtained by FFT spectrum analysis. Moreover, using spectrum averaging technique on  $g(t)$  can further improve the estimation accuracy of  $\hat{f}_0$ .

## 4. Numerical Simulation

In this section, SNR and successful detection rate (SDR) are used to evaluate the effectivity of proposed algorithm. SNR is defined as

$$\text{SNR} = 20 \log_{10}\left(\frac{A}{\sqrt{2D}}\right),$$

where  $D$  is noise intensity. Without loss of generality, the LFM signal in Eq.(7) is parameterized with  $A=0.5V$ ,  $f_0=2\text{Hz}$ ,  $k=0.001\text{Hz/s}$ .

### 4.1 Estimation of Chirp Rate $k$

Choose sampling time  $T_1=1000\text{s}$ , SR system parameters  $a=b=1$ , segment number  $M=50$  and segment length  $T=20\text{s}$ . According to the preprocess of step1~step3, the smoothed signal  $s_1(t)$  with theoretic frequency  $KT=0.02\text{Hz}$  is given as

$$\begin{aligned} s_1(t) &= 0.25 \cos(2\pi \times 0.02t + 39.8) \\ &\quad + \frac{1}{50} \sum_{m=0}^{49} \text{Re}(P_m(t + 20m)) \end{aligned} \quad (14)$$

Input  $s_1(t)$  into SR system as mentioned in step4, and the spectrum of output of SR system is depicted in Fig.2. The result shows that there is a clear spectrum peak located at 0.02Hz under the condition of SNR = -20dB, the chirp rate is thus estimated as  $\hat{k} = 0.02 / T = 0.02 / 20 = 0.001 \text{ Hz/s}$ .

Consider the negative effect on parameter estimation caused by noise in low SNR environment, we exploit the spectrum averaging technique to decrease the estimation error and thus improve the estimation accuracy. Using 40 times of spectrum averaging on output signal of SR system, the estimation results of chirp rate are listed in Table 1. The data show that the estimated chirp rate very closes to its true value ( $k=1.0 \times 10^{-3} \text{ Hz/s}$ ) when  $\text{SNR} \geq -20\text{dB}$ , and the chirp rate estimation is accurate at the cost of moderately increasing the times of spectrum averaging.

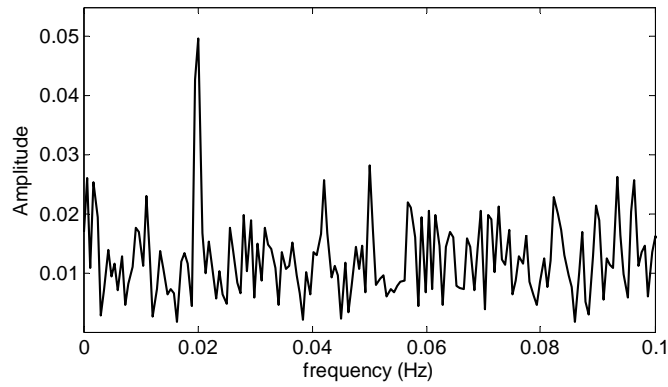


Figure 2. The frequency spectrum of output of SR in step4 under the condition of SNR=-20dB

TABLE I. THE ESTIMATION RESULTS OF CHIRP RATE USING 40 TIMES OF SPECTRUM AVERAGING ( $k=1.0 \times 10^{-3}$  Hz/s)

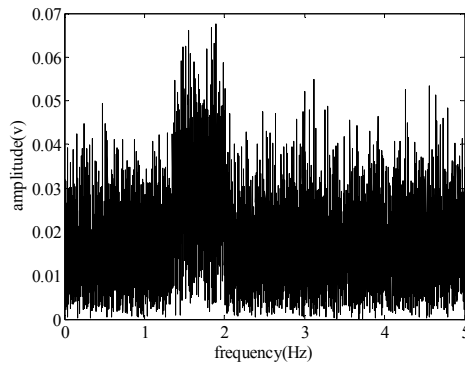
SNR (dB)	-22	-21	-20	-19
$\hat{k}$ (Hz/s)	$1.3 \times 10^{-3}$	$1.005 \times 10^{-3}$	$1.000 \times 10^{-3}$	$1.000 \times 10^{-3}$

#### 4.2 Estimation of Initial Frequency $f_0$

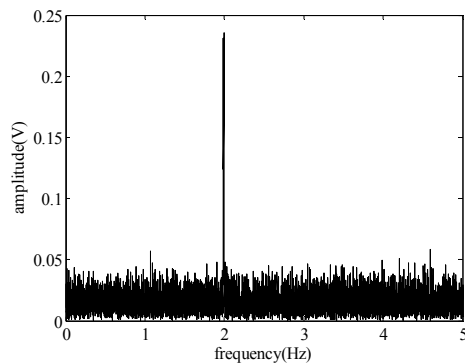
Once the chirp rate  $\hat{k}$  has been estimated in step4,  $g(t)$  can be constructed according to step5 as follows:

$$g(t) \approx 0.5 \cos(2\pi f_0 t) + \text{Re}(\exp(-j\pi \hat{k} t^2) n(t)).$$

Unlike the chirp rate estimation where we resort to SR, here we only use FFT spectrum analysis of  $g(t)$  to estimate  $f_0$ , the initial frequency of LFM. Similarity, using spectrum averaging technique on  $g(t)$  can further improve the estimation accuracy of  $f_0$ .



(a) SNR=-22dB



(b) SNR=-21dB

Figure 3. The 10 times of spectrum averaging of reconstructed  $g(t)$

Figure 3 gives the averaging spectrum of reconstructed  $g(t)$  based on the chirp rate estimation  $\hat{k}$ . As can be seen from Fig.3(a) where SNR=-22dB, we can not estimate  $f_0$  by spectrum averaging technique. While in the case of SNR=-21dB, there is a clear peak located at 2Hz as depicted in Fig.3(b), thus the initial frequency  $f_0$  can be successfully estimated. Further simulations are performed under SNR= -22dB~-19dB using 20 times of spectrum averaging, and the estimation results are summarized in Table II. The data of Table II shows that the initial frequency  $f_0$  can be accurately estimated when SNR $\geq$ -20dB.

TABLE II. THE INITIAL FREQUENCY ESTIMATION USING 20 TIMES OF SPECTRUM ABERAGING ( $f_0=2$  Hz)

SNR(dB)	-22	-21	-20	-19
$\hat{f}_0$ (Hz)	1.7929	1.9957	2.002	2.002

### 4.3 Performance Analysis

To evaluate the reliability of parameter estimation, the Monte-Carlo-based successful detection rate (SDR) is introduced. Here we refer to a successful detection if the relative estimation error less than 2%, i.e. if the estimated  $\hat{k}$  falls in interval  $[0.98 \times k, 1.02 \times k]$  during one detection, a successful detection happens. Since  $f_0$  is estimated at the condition of estimation of  $k$ , it is sufficient to evaluate the SDR of chirp rate  $k$ .

Figure 4 illustrates the relationship of SDR of chirp rate with respect to SNR and the times of spectrum averaging (1000 Monte-Carlo simulations). From Fig.4 we can see that the more the times of spectrum averaging is, the higher the SDR of chirp rate and the lower the detection SNR will be. For 10 times of spectrum averaging, the detection SNR can achieves to -19dB in the constraint of SDR=100%, while for 40 times of spectrum averaging the lowest detection SNR achieves down to -21dB.

The relationship of SDR and segment number  $M$  is further exploited, which is depicted in Fig.5. From the data of Fig.5, it demonstrates that the more the times of spectrum averaging is, the higher the SDR of chirp rate will be, which is similar to Fig.4. Significantly, the SDR is improved obviously with the increasing of segment number  $M$ . The improvement rate of SDR increases faster when  $M$  is small, whereas it increases slower when  $M$  is larger than 50. Since the computational load of algorithm will be increased with the increasing of  $M$ ,  $M$  will be selected approximately to 50 on the consideration of cost performance.

In addition, the detection SNR and the accuracy of parameter estimation of proposed algorithm are compared with that of other algorithms, as listed in Table III. The data show that the proposed algorithm exhibits very good detection performance achieving to  $10^{-3}$  estimation accuracy at very low SNR, which outperforms the detection ability of FRFT, HHHT and LHT based algorithms, whose lowest detection SNR is only above -12dB.

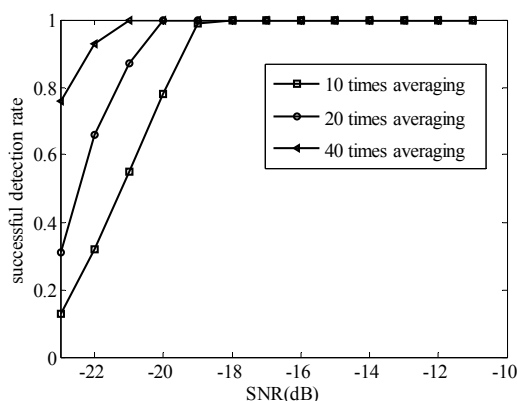


Figure 4. The successful detection rate of chirp rate with respect to the times of spectrum averaging and SNR. (2% relative estimation error, segment number  $M=50$ )

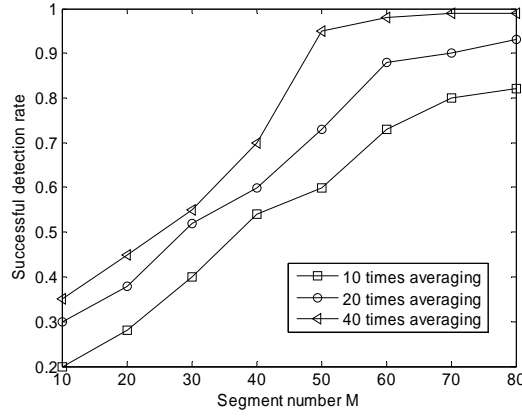


Figure 5. The successful detection rate of chirp rate with respect to segment number M and the times of spectrum averaging (2% relative estimation error, SNR = -20dB)

TABLE III. THE COMPARISON OF DETECTION SNR AND ESTIMATION ACCURACY

	Detection SNR (dB)	Estimation accuracy	
		chirp rate $k$	Initial frequency $f_0$
FRFT <sup>[4]</sup>	-12	$10^{-3} \sim 10^{-2}$	$10^{-3} \sim 10^{-2}$
HHHT <sup>[5]</sup>	-3	$10^{-1}$	$10^{-2}$
LHT <sup>[6]</sup>	-11	$10^{-3}$	$10^{-2}$
This paper	-20	$10^{-3}$	$10^{-3}$

## 5. Conclusion

This paper presents a novel method to detect and estimate LFM signal based on SR system. Utilizing the segmented correlation smoothing and the spectrum averaging techniques, the proposed method can accurately estimate the chirp rate and the initial frequency of LFM in the condition of  $\text{SNR} \geq -20\text{dB}$ . The achieved SNR of parameter estimation is much lower than that of time-frequency analysis methods, such as FRFT, STFT and WV based methods, and it does not require a prior knowledge of parameter range of LFM signal. Simulation results show the effectiveness of proposed algorithm for LFM signal detection and estimation under very low SNR.

## 6. Acknowledgment

This work was supported by the Excellent Youth Foundation of Sichuan Province (Grant No. 2011JQ0027), the Fundamental Research Funds of Southwest Jiaotong University (Grant No. 2008B08), partly by the National Natural Science Foundation of China (Grant No. 60903202), the Specialized Research Fund for the Doctoral Program of Higher Education of China (Grant No. 20090184120024), and the Fundamental Research Funds for the Central Universities (Grant No. SWJTU11CX041)

## 7. References

- [1] M. S. Wang, A. K. Chan, and C. K. Chui, Linear frequency -modulated signal detection using randon-ambiguity transform, IEEE Trans. on Signal Processing, 46(3), pp. 571-586,1998.
- [2] S. Barbarossa, Analysis of multicomponent LFM signals by a combined Wigner-Hough transform, IEEE Trans. Signal Process. 43 (6), pp.1511-1515, 1995.
- [3] Y. Sun, P. Willett, Hough transform for long chirp detection, IEEE Trans. on Aerospace and Electronic Systems, 38 (2), pp.553-569, 2002.

- [4] L. Qi, R. Tao, S. Zhou, et al., Detection and estimation of multicomponent LFM signals based on fractional Fourier transform, *Science in China (Series E)*, 3 (8), pp. 749-759, 2003.
- [5] Yuan Ye, Qing-fu Li, Ying Fu. Detection and parameter estimation of multicomponent LFM signals based on Hilbert-Huang Hough Transform. the 2nd Asia-Pacific Conference on Computational Intelligence and Industrial Applications, China, 1:476-479, 2009.
- [6] G. Bi, X. Li, C.M. See, LFM signal detection using LPP-Hough transform, *Signal Processing*, 91, pp.1432-1443, 2011.
- [7] X. Lv, M. Xing, S. Zhang, Z. Bao, Keystone transformation of the Wigner-Ville distribution for analysis of multicomponent LFM signals, *Signal Processing*, 89, pp.791-806, 2009.
- [8] R. Benzi, A. Sutera, and A. Vulpian. The mechanism of stochastic resonance, *Journal of Physics*, 14(11), pp.453-457, 1981.
- [9] Q. Li, T. Wang, Y. Leng, W. Wang, G. Wang, Engineering signal processing based on adaptive step-changed stochastic resonance, *Mechanical Systems and Signal Processing*, 21, pp.2267-2270, 2007.
- [10] F. Duan, D. Abbott, Signal detection for frequency-shift keying via short-time stochastic resonance, *Physics Letters A*, 344, pp.401-410, 2005.
- [11] B. Xu, F. Duan, R. Bao, J. Li, Stochastic resonance with tuning system parameters: the application of bistable systems in signal processing, *Chaos, Solitons and Fractals*, 13, pp. 633-644, 2002.